



Original research

Qualitative evaluation of anterior segment in angle closure disease using anterior segment optical coherence tomography

Sasan Moghimi^{a,b,*}, Rebecca Chen^b, Nikoo Hamzeh^a, Nassim Khatibi^a, Shan C. Lin^b

^a Farabi Eye Hospital, Tehran University of Medical Sciences, Tehran, Iran

^b Koret Vision Center, University of California, San Francisco Medical School, San Francisco, CA, USA

Received 12 April 2016; revised 22 June 2016; accepted 22 June 2016

Available online 12 July 2016

Abstract

Purpose: To evaluate different mechanisms of primary angle closure (PAC) and to quantify anterior chamber (AC) parameters in different subtypes of angle closure disease using anterior segment optical coherence tomography (AS-OCT).

Methods: In this prospective study, 115 eyes of 115 patients with angle closure disease were included and categorized into three groups: 1) fellow eyes of acute angle closure (AAC; 40 eyes); 2) primary angle closure glaucoma (PACG; 39 eyes); and 3) primary angle closure suspect (PACS; 36 eyes). Complete ophthalmic examination including gonioscopy, A-scan biometry, and AS-OCT were performed. Based on the AS-OCT images, 4 mechanisms of PAC including pupillary block, plateau iris configuration, thick peripheral iris roll (PIR), and exaggerated lens vault were evaluated. Angle, AC, and lens parameter variables were also evaluated among the three subtypes.

Results: There was a statistically significant difference in the mechanism of angle closure among the three groups ($p = 0.03$). While the majority of fellow eyes of AAC and of PACS eyes had pupillary block mechanism (77.5% and 75%, respectively), only 48.7% of PACG eyes had dominant pupillary block mechanism ($p = 0.03$). The percentage of exaggerated lens vault and plateau iris mechanisms was higher in PACG eyes (25.5% and 15.4%, respectively). Fellow eyes of AAC had the shallowest AC ($p = 0.01$), greater iris curvature ($p = 0.01$), and lens vault ($p = 0.02$) than PACS and PACG eyes. Iris thickness was not significantly different among the three groups ($p = 0.45$).

Conclusion: Using AS-OCT, we found that there was a statistically significant difference in the underlying PAC mechanisms and quantitative AC parameters among the three subtypes of angle closure disease.

Copyright © 2016, Iranian Society of Ophthalmology. Production and hosting by Elsevier B.V. This is an open access article under the CC BY-NC-ND license (<http://creativecommons.org/licenses/by-nc-nd/4.0/>).

Keywords: Anterior segment optical coherence tomography; Angle closure; Glaucoma; Lens vault; Iris curvature

Introduction

Primary angle closure glaucoma (PACG) is a major cause of blindness worldwide, accounting for bilateral blindness in more than almost 5.3 million people by 2020.¹ Although pupillary block and plateau iris syndrome have been proposed as the two main mechanisms in the pathogenesis of angle closure disease, other anatomical factors related to the iris, lens, and ciliary body have also been shown to play important roles.^{2–5} Established ocular biometric factors associated with angle closure disease include a shorter axial length (AL), shallower anterior chamber (AC), thicker peripheral iris, and a thicker, more anteriorly positioned lens.^{5–10}

The article has been presented as poster in 5th World Glaucoma Congress 2013 – Vancouver Canada.

The authors did not receive any financial support from any public or private sources.

The authors have no financial or proprietary interest in a product, method, or material described herein.

* Corresponding author. Farabi Eye Research Center, Tehran University of Medical Sciences, Quazvin Sq., Tehran, Iran.

E-mail address: sasanimii@yahoo.com (S. Moghimi).

Peer review under responsibility of the Iranian Society of Ophthalmology.

With the development of anterior segment optical coherence tomography (AS-OCT), researchers can capture and visualize the entire anterior segment in a single image and assess angle, iris, and lens parameters. AS-OCT-based parameters, such as lens vault, AC area, AC width, and iris thickness have been associated with angle closure.^{11–13} Iris curvature has been proposed to be an indicator of pupillary block.^{4,14–16} As iris curvature is reported to be only moderately correlated with increased lens vault, pupillary block may not be the only mechanism by which increased lens vault causes angle closure.^{10,14} In fact, there are some cases with exaggerated lens vault in which the iris appears to drape the anterior surface of the lens, giving rise to a “volcano-like configuration” without an increase in iris curvature.^{3,17,18}

Shabana et al³ evaluated four different mechanisms of primary angle closure (PAC) using AS-OCT. In their new classification, AS-OCT images were categorized into four mechanisms including pupillary block, plateau iris configuration, thick peripheral iris roll (PIR), and exaggerated lens vault.

Angle closure disease is classified into different subtypes including primary angle closure suspect (PACS), acute angle closure (AAC), and PACG.^{17,19,20} Qualitative and quantitative evaluation of the anterior segment in these eyes might be helpful in explaining the pathogenesis of angle closure. Understanding these mechanisms may explain why some of these eyes develop AAC while others lead to chronic disease. Our previous studies^{9,10,13,18} have shown that exaggerated lens vault is one of the main mechanisms in eyes with AAC during attack. In this study, different subtypes of angle closure disease including fellow eyes of AAC, PACG, and PACS were evaluated.

Methods

Patients

In this cross-sectional study, between Sep 2011 and Sep 2013, 154 eyes (154 patients) with at least one eye with AAC, PACS status, and PACG, as defined below, were consecutively recruited from the Glaucoma Clinic, a tertiary care center of the Farabi Eye Hospital, prior to a laser iridotomy. The Ethics Committee at Farabi Eye Hospital approved the study protocol. All patients provided written informed consent forms in accordance with the Declaration of Helsinki. Only the right eyes of patients were included for analysis in this study. If the left eye was the only affected one, the left eye was included. Eyes with a history of pilocarpine usage, trauma, uveitis, ocular laser, and/or surgical procedures (e.g., laser peripheral iridotomy; LPI) were excluded. Additionally, we excluded eyes with pseudoexfoliation (PEX), iris or angle neovascularization, any kind of secondary angle closure, or any iris or corneal abnormalities. None of the patients had taken any miotic or mydriatic medications.

After excluding eyes with poor AS-OCT image quality (28 eyes), PEX (4 eyes), prior LPI (3 eyes), and secondary angle closure (2 eyes), a total of 115 eyes (115 patients) were classified into one of the following three groups:

- 1) The fellow eye of AAC (40 eyes). AAC was defined as: a) at least two of the symptoms of an acute episode of intraocular pressure (IOP) rise which are ocular pain or headache, nausea and/or vomiting, decreased vision, and rainbow-colored halos around lights; b) IOP at presentation of at least 30 mmHg with Goldmann applanation tonometry; c) examination findings such as conjunctival injection, corneal epithelial edema, fixed mid-dilated pupil, and shallow AC; and d) shallow AC and narrow angle in the other eye.
- 2) PACG eyes (39 eyes) had chronically elevated IOP above 21 mmHg (prior to treatment) along with glaucomatous optic neuropathy and characteristic visual field defects, shallow AC, and iridotrabecular contact (ITC) in at least 3 quadrants on gonioscopy along with a variable amount of peripheral anterior synechiae (PAS).
- 3) PACS eyes (36 eyes) were classified based on the posterior trabecular meshwork not being visible in at least 3 quadrants without PAS or any evidence of glaucomatous optic nerve or visual field damage. These patients did not have any history or sign of previous AAC attack, and IOP was ≤ 21 mmHg without medication.

Exams

Slit lamp examination of the anterior segment, Goldmann applanation tonometry, and gonioscopy in dark conditions (with and without indentation) were conducted in all patients. Indentation gonioscopy was performed by a glaucoma specialist (S.M.) using a Zeiss-style four-mirror gonioscope (Model G-4, Volk Optical, Mentor, OH), and the angles were graded using Shaffer system. A-scan biometry (Echoscan, model U3300, Nidek, Tokyo, Japan) was used to measure AL, lens thickness (LT), and anterior chamber depth (ACD).

All subjects underwent static automated white-on-white threshold perimetry (program 24-2, Swedish Interactive Threshold Algorithm standard, model 750, Humphrey Field Analyzer, Humphrey Instruments, Dublin, CA).

Anterior segment optical coherence tomography

AS-OCT (Visante OCT; Carl Zeiss Meditec, Dublin, CA) was performed for all the patients in the dark. Scans were centered on the pupil and were obtained along the horizontal and vertical axes using the enhanced anterior segment single protocol. Two images were captured for each axis, and the one with higher quality was chosen for analysis. Detection of the scleral spurs was optimized by adjusting the brightness and contrast of each image. Two experienced ophthalmologists (S.M., N.H.) determined the location of the scleral spur

in each image, and all images were validated for image quality and scleral spur location by the principal investigator (S.M.). Table 1 lists the definitions of the parameters measured using the Visante OCT software (version 2.0.1.88).^{11,16,21} Parameters which were measured on both the nasal and temporal sides of the eye, including angle opening distance at 750 μm from scleral spur, trabeculo-iris space area at 750 μm from scleral spur, AC angle, iris curvature, and iris thickness, are represented by the mean values of the nasal and temporal values.

Qualitative analysis of an AS-OCT image

Only images with clearly discernible scleral spurs were analyzed qualitatively by two glaucoma specialists (A.L.C., S. S. L.) who were masked to the clinical categories and clinical findings. All images were categorized into four groups based on PAC mechanisms (Fig. 1)³: 1) **Pupillary Block** was defined as eyes with an anteriorly convex iris profile, a small central zone of iridolenticular contact, and shallow peripheral AC, with a typical bombe appearance; 2) **Plateau Iris** was defined as eyes in which the iris root rises steeply from its insertion and angles downward from the angle wall and in which there are a central flat iris plane and deep AC; 3) **Thick Peripheral Iris Roll (Thick PIR)** was defined as eyes in which prominent circumferential folds of the peripheral iris occupy a large part of the angle; 4) **Exaggerated Lens Vault** was defined as eyes with a “volcano-like configuration” of the iris and small AC volume secondary to anterior displacement of the iris by the lens. The iris appears to drape over the anterior surface of the lens, and the space between iris surface and endothelium is markedly decreased.

Where images revealed more than one mechanism of PAC, the dominant (primary) and secondary mechanisms of angle closure was determined. When the two glaucoma specialists did not agree, a third glaucoma specialist (S.M.) was the arbitrator.

Table 1
Anterior segment parameters measured by anterior segment optical coherence tomography and their definitions.

Parameter	Definition
Anterior Chamber Depth (ACD)	The axial distance from the corneal endothelium to the anterior lens surface.
Anterior Chamber Width (ACW)	The distance between the 2 scleral spurs.
Anterior chamber angle (ACA)	The trabecular–iris angle measured with the apex in the iris recess and the arms of the angle passing through a point on the trabecular meshwork at 500 μm from the scleral spur and the point on the iris perpendicularly opposite 5.
Angle Opening Distance at 750 μm (AOD750)	The distance between the posterior corneal surface and the anterior iris surface on a line perpendicular to the trabecular meshwork, 750 μm from the scleral spur.
Trabecular Iris Space Area at 750 μm (TISA750)	The surface area of a trapezoid with the following boundaries: anteriorly, the angle opening distance at 750 μm from scleral spur; posteriorly, a line drawn from the scleral spur perpendicular to the plane of the inner scleral wall to the iris; superiorly, the inner corneoscleral wall; and inferiorly, the iris surface.
Iris Curvature (I-Curve)	The perpendicular distance from a line between the most central to the most peripheral points of the iris pigment epithelium to the posterior iris surface at the point of greatest convexity.
Iris Thickness (IT)	Iris thickness at 750 μm from the scleral spur (IT750).
Lens Vault (LV)	The perpendicular distance from the anterior pole of the lens to the horizontal line between the scleral spurs.

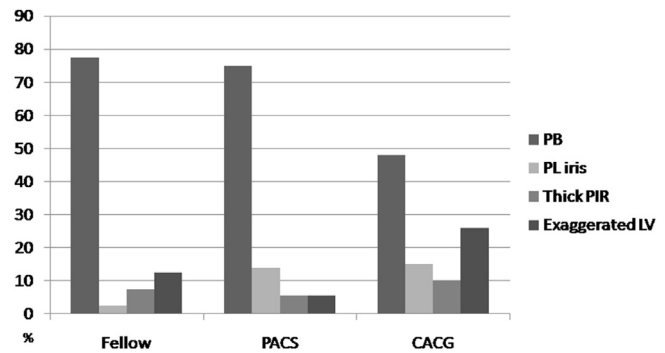


Fig. 1. Nasal-temporal anterior segment optical coherence tomography images showing four mechanisms of primary angle closure Pupillary Block (A), Plateau iris (B), Dominant thick peripheral iris roll and pupillary block as secondary mechanism (C), and Exaggerated Lens Vault (D).

All enrolled eyes with angle closure received LPI, which is the standard of care. After pupillary dilation, the density of the crystalline lens nucleus was graded by the Lens Opacities Classification System III (LOCS III).²² The clinical examiners were not masked for crystalline lens opacification grading. A dilated fundus examination including stereoscopic examination of the optic nerve head was performed on all enrolled eyes.

Statistical analysis

Statistical analysis was performed using SPSS software version 17 (SPSS, Inc., Chicago, IL).

Continuous variables are expressed as mean \pm standard deviation (SD). ANOVA and post hoc Tukey tests were used for analysis of parametric variables. Nonparametric variables were analyzed by the Kruskal-Wallis test. Chi-square testing was used for analysis of qualitative variables. The inter-observer and intra-observer agreement among the glaucoma specialists in classification of images were assessed by Kappa (k) statistics. p values less than 0.05 were considered statistically significant.

Results

The demographic and clinical examination data of the three groups are summarized in Table 2. There was no difference in age and gender among these groups. As would be expected, the IOP was significantly greater in PACG eyes than the other groups, even with the use of anti-glaucoma medications ($p < 0.001$). These eyes also had a larger cup-to-disc ratio ($p < 0.001$) (Table 2). For classification of images, inter-observer agreement (kappa coefficient) was 0.91 and intra-observer agreement was 0.89–0.97, respectively. For 12 images, a third expert needed to be the arbitrator.

Gonioscopically, the AC angle was narrowest in the fellow eyes, followed by eyes with PACG and PACS. However, the difference did not reach statistical significance. ACA, AOD750, and TISA750 were significantly less in fellow eyes and the PACG group than the PACS group (Table 3; $p < 0.001$ for all).

The eyes with PACS had similar ACD as PACG eyes (2.53 ± 0.28 vs. 2.49 ± 0.25 , respectively, $p = 0.97$), but had deeper AC than fellow eyes in the AAC group (2.36 ± 0.21 , $p < 0.04$; Tables 3 and 4). The lens vault was highest ($977.00 \pm 192.32 \mu\text{m}$) in fellow eyes followed by PACS eyes; the lowest lens vault was observed in PACG eyes ($851.28 \pm 186.65 \mu\text{m}$, $p < 0.001$). There was no statistically significant difference in the mean IT750 among the three groups ($p = 0.45$) (Table 4); however, iris curvature was greater in fellow eyes (0.29 ± 0.09), followed by PACS eyes (0.27 ± 0.08) and PACG eyes (0.27 ± 0.08) ($p = 0.01$).

Qualitative evaluation

Seventy-seven eyes (67.0%) had pupillary block, 17 eyes (14.8%) had lens vault, 12 eyes (10.4%) had thick PIR, and 9 eyes (7.8%) had plateau iris as the dominant mechanism (Table 5). The mechanism of ACG differed significantly between fellow eyes of AAC, eyes with PACG, and eyes with

Table 2
Comparison of demographic and clinical examination data in angle closure subtypes.

	Fellow eye	PACG	PACS	p-value
No. Eyes	40	39	36	–
Age (years), mean \pm SD	59.4 \pm 9.2	60.7 \pm 9.0	60.2 \pm 8.1	0.86
Female/Male	31/9	20/19	27/9	0.09
IOP (mm Hg), mean \pm SD	12.7 \pm 3.2	20.8 \pm 7.4	15.8 \pm 2.6	<0.001
Medication number, mean \pm SD	1.0 \pm 0.7	1.7 \pm 1.3	0.0 \pm 0.0	<0.001
C/D ratio, mean \pm SD	0.30 \pm 0.11	0.68 \pm 0.21	0.29 \pm 0.09	<0.001
Gonioscopy (Shaffer grading system), mean \pm SD	0.44 \pm 0.55	0.54 \pm 0.59	0.64 \pm 0.57	0.31
PAS (degrees), mean \pm SD	13.1 \pm 32.6	184.0 \pm 146.9	0.0 \pm 0.0	<0.001
Lens nucleus opacity (per LOCS III), mean \pm SD	2.5 \pm 0.7	2.7 \pm 0.9	2.6 \pm 0.9	0.32

PACG: primary angle closure glaucoma; **PACS:** primary angle closure suspect; **C/D:** cup-to-disc; **IOP:** intraocular pressure; **PAS:** peripheral anterior synechiae; **LOCS III:** lens opacities classification system III.

Table 3
Angle, anterior chamber, and lens parameters of subtypes of angle closure and normal control eyes measured by anterior segment optical coherence tomography or A-scan ultrasound.

Parameters	Fellow eye	PACG	PACS	p-value
AOD750 (mm)	0.074 \pm 0.043	0.113 \pm 0.083	0.146 \pm 0.088	<0.001
TISA750 (mm ²)	0.036 \pm 0.022	0.047 \pm 0.038	0.082 \pm 0.040	<0.001
ACA (degree)	3.19 \pm 2.73	5.00 \pm 4.81	8.96 \pm 5.08	<0.001
Lens thickness (mm)	4.96 \pm 0.32	4.86 \pm 0.40	4.92 \pm 0.30	0.48
ACD (mm)	2.36 \pm 0.21	2.49 \pm 0.25	2.53 \pm 0.28	0.01
Axial length (mm)	21.69 \pm 1.13	22.48 \pm 0.82	21.97 \pm 0.73	0.001
Lens vault (μm)	977.00 \pm 192.32	851.28 \pm 186.65	890.25 \pm 221.30	0.02
I-Curve (mm)	0.29 \pm 0.09	0.22 \pm 0.11	0.27 \pm 0.08	0.01
IT750(mm)	0.47 \pm 0.09	0.44 \pm 0.08	0.46 \pm 0.12	0.45

PACG: primary angle closure glaucoma; **PACS:** primary angle closure suspect; **AOD750:** average of nasal and temporal angle opening distance at 750 μm from scleral spur; **TISA750:** average of nasal and temporal trabeculo-iris space area at 750 μm from scleral spur; **ACA:** average of nasal and temporal anterior chamber angle; **ACD** = anterior chamber depth; **I-curve:** average of nasal and temporal iris curvature; **IT750:** average of nasal and temporal iris thickness at 750 μm from scleral spur. Significant P values are demonstrated in bold.

Table 4
Pairwise comparison of anterior chamber and lens parameters among different subtypes of angle closure disease.

Parameters	Glaucoma subtype	Fellow eye	PACG
Lens vault (p-value)	PACG	0.01	–
	PACS	0.13	0.66
I-curve (p-value)	PACG	0.01	–
	PACS	0.14	0.63
IT750 (p-value)	PACG	0.42	–
	PACS	0.72	0.84
ACD (p-value)	PACG	0.19	–
	PACS	0.04	0.97

PACG: primary angle closure glaucoma; **PACS:** primary angle closure suspect; **LV:** lens vault; **ACD:** anterior chamber depth, **I-curve:** average of nasal and temporal iris curvature; **IT750:** average of nasal and temporal iris thickness at 750 μm from scleral spur. Significant P values are demonstrated in bold.

Table 5
Qualitative analysis of anterior segment optical coherence tomography images for dominant and secondary mechanisms showing a significant difference ($p = 0.03$) in primary mechanism among fellow eyes of acute angle closure glaucoma, primary angle closure glaucoma eyes, and primary angle closure glaucoma eyes.

Glaucoma subtypes		Pupillary block	Plateau iris	Thick PIR	Exaggerated LV
PACG (%)	Dominant	19 (48.7)	6 (15.4)	4 (10.3)	10 (25.6)
	Secondary (12 eyes)	2 (5.1)	–	6 (15.3)	4 (10.3)
PACS (%)	Dominant	27 (75.0)	2 (5.6)	5 (13.9)	2 (5.6)
	Secondary (11 eyes)	1 (2.8)	–	4 (11.1)	6 (16.6)
Fellow eye (%)	Dominant	31 (77.5)	1 (2.5)	3 (7.5)	5 (12.5)
	Secondary (12 eyes)	2 (5.0)	1 (2.5)	1 (2.5)	8 (20)

PACG: primary angle closure glaucoma; **PACS:** primary angle closure suspect; **LV:** lens vault; **PIR:** peripheral iris roll.

PACS ($p = 0.03$). While pupillary block was the dominant mechanism in the majority of fellow and PACS eyes (77.5% and 75%, respectively), only 48.7% of PACG eyes had pupillary block (Table 4). Instead, PACG eyes had relatively higher proportions of exaggerated lens vault and plateau iris as the dominant mechanism (25.5% and 15.4%, respectively). Overall, PACS eyes had a similar pattern of mechanisms as fellow eyes of AAC (Fig. 2). PACG eyes, PACS eyes, and fellow eyes of AAC had 12, 11, and 12 secondary mechanisms, respectively (Table 5).

Discussion

In the present study, pupillary block appears to be the dominant mechanism of angle narrowing in fellow eyes of AAC eyes and in PACS eyes. In eyes with PACG, about a half of the eyes did not have dominant pupillary block and instead demonstrated plateau iris configuration, exaggerated lens vault, or thick peripheral iris.

Anatomical predispositions such as shallow AC, short AL, small corneal diameter, and thick and more anteriorly positioned crystalline lens are considered major risk factors for the development of PACG.^{6,23,24} A shallow AC is the most important and consistent biometric feature predisposing to AAC in studies involving multiple ethnicities.^{4,25–29} Fellow eyes of AAC have been considered to be a “pre-attack stage”,^{30,31} as up to half of these eyes will also develop an AAC attack within five years if left untreated.^{25,27} Consistent with the results of Friedman et al, fellow eyes of AAC eyes have shallower AC than do PACS eyes. However, ACD was not significantly different between eyes with PACS and PACG. This finding might be justified by a higher percentage of plateau iris and prominent iris roll in our PACG group.

Pupillary block has been proposed as the main mechanism of angle closure in most studies. Prophylactic LPI has been shown to be safe and effective in preventing AAC attack in fellow eyes. Three fourths of fellow eyes of AAC eyes had pupillary block as the main mechanism for angle closure, and the highest iris curvature was seen in this group. Relief of pupillary block may explain why PI is effective in these eyes.

Lens vault is another anatomical factor that has been associated with the development of angle closure disease.¹¹

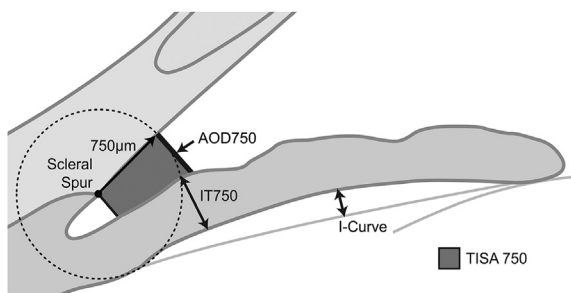


Fig. 2. Qualitative analysis of AS-OCT images shows a significant difference ($p = 0.03$) among fellow eyes of acute angle closure glaucoma, primary angle closure glaucoma and primary angle closure glaucoma eyes in terms of dominant mechanism.

Studies in Chinese, Japanese, Iranian, and Singaporean ethnicities have confirmed the role of LV in different subtypes of angle closure.^{4,10,11,14,28} Our results show that the fellow eyes of AAC eyes have greater LV than do other groups, especially when compared to PACG eyes. A greater LV may increase the chance of AAC by pushing the iris anteriorly. Recent studies have addressed a category of eyes with exaggerated LV in which the iris appears to drape over the anterior surface of the lens, giving rise to a “volcano-like configuration” without any increase in iris curvature.³ In our patients, iris thickness was not thicker in eyes with pupillary block or exaggerated lens vault. Although anterior protrusion of the lens may increase iridolenticular contact and lengthen and narrow the iris-lens channel, causing pupillary block,^{5,11} a better explanation in these cases of exaggerated LV may be that the direct anterior push on the iris crowds the angle. Greater LV may predispose the eye to angle closure through multiple mechanisms.^{5,11} A considerable proportion of PACG (25%) and fellow eyes of AAC (12.5%) in this study had exaggerated LV without significant iris curvature. The effect of LPI in eyes and with pure exaggerated LV has not been evaluated, and cataract surgery may be a better option in these eyes.

Thick “prominent iris roll” (PIR) has been used to describe a subclass of non-pupillary block in which prominent circumferential folds at the base of the iris enlarge during dilation and may come into contact with trabecular meshwork.⁷ A recent review describing angle closure mechanisms using AS-OCT suggested that 15% of angle closure may be attributed to PIR.³ In the present study, thick PIR was the predominant mechanism for angle closure in 7.5% of fellow eyes of AAC, 13.9% of PACS eyes, and 10.3% of PACG eyes, demonstrating a similar proportion among all three groups. As in plateau iris syndrome, LPI is ineffective in patients with thick PIR.^{7,32,33}

Angle closure typically occurs in the setting of one or a combination of several anatomic risk factors. Nongpiur et al recently described three distinct subgroups in a cluster analysis of PACS eyes based on AS-OCT imaging.²¹ The first subgroup was characterized by a large iris area; the second subgroup was characterized by a large LV and shallow ACD; and the third subgroup was characterized by elements of both other subgroups.

In the present study, the patterns of angle-narrowing mechanisms in PACS and fellow eyes of AAC are similar, with a more crowded AC in fellow eyes, but PACG eyes demonstrate different mechanisms from those of PACS eyes or fellow eyes of AAC. Our finding that half of PACG eyes have pupillary block is consistent with Yao et al and Kumar et al,^{34,35} who reported that one-third of PACS and fellow eyes of AAC had plateau iris syndrome based on standardized ultrasound biomicroscopic (UBM) criteria. These findings suggest that non-pupillary block mechanisms such as angle crowding secondary to a thick iris, an anteriorly directed iris, or an anteriorly displaced lens play important roles in developing chronic disease while pupillary block is the dominant mechanism in AAC.

Our study had some limitations. The study was hospital-based rather than population-based, and therefore, the observed results may not be generalized to larger populations. Another limitation was that we did not perform UBM in our patients to diagnose plateau iris configuration more precisely. While some other studies have defined plateau iris configuration based on AS-OCT images, plateau iris syndrome can only be diagnosed definitively with UBM or indentation gonioscopy after LPI. Lastly, although we used standardized criteria to categorize eyes by the major mechanism of angle narrowing, in some cases, two or more mechanisms may be responsible for disease.

In conclusion, this study qualitatively reports AC morphology in different subgroups of angle closure patients. Although there appear to be several anatomical mechanisms for angle narrowing or closure, pupillary block is responsible for the majority of angle narrowing in PACS eyes and in fellow eyes of AAC, as well as in half of PACG eyes. AS-OCT imaging may help us better predict which eyes are more likely to benefit from an iridotomy to relieve pupillary block and which eyes are not, such as eyes with PACG.

References

1. Quigley HA, Broman AT. The number of people with glaucoma worldwide in 2010 and 2020. *Br J Ophthalmol.* 2006;90:262–267.
2. Niwas SI, Lin W, Bai X, et al. Reliable feature selection for automated angle closure glaucoma mechanism detection. *J Med Syst.* 2015;39:1–10.
3. Shabana N, Aquino MCD, See J, et al. Quantitative evaluation of anterior chamber parameters using anterior segment optical coherence tomography in primary angle closure mechanisms. *Clin Exp Ophthalmol.* 2012;40:792–801.
4. Sng CC, Aquino MCD, Liao J, et al. Pretreatment anterior segment imaging during acute primary angle closure: insights into angle closure mechanisms in the acute phase. *Ophthalmology.* 2014;121:119–125.
5. Tarongoy P, Ho CL, Walton DS. Angle-closure glaucoma: the role of the lens in the pathogenesis, prevention, and treatment. *Surv Ophthalmol.* 2009;54:211–225.
6. George R, Paul P, Baskaran M, et al. Ocular biometry in occludable angles and angle closure glaucoma: a population based survey. *Br J Ophthalmol.* 2003;87:399–402.
7. He M, Foster P, Johnson G, Khaw P. Angle-closure glaucoma in East Asian and European people. Different diseases? *Eye.* 2005;20:3–12.
8. Lavanya R, Wong TY, Friedman DS, et al. Determinants of angle closure in older Singaporeans. *Arch Ophthalmol.* 2008;126:686–691.
9. Moghimi S, Torabi H, Hashemian H, Amini H, Lin S. Central corneal thickness in primary angle closure and open angle glaucoma. *J Ophthalmic Vis Res.* 2014;9:439–443.
10. Moghimi S, Vahedian Z, Fakhraie G, et al. Ocular biometry in the subtypes of angle closure: an anterior segment optical coherence tomography study. *Am J Ophthalmol.* 2013;155:664–673. e1.
11. Nongpiur ME, He M, Amerasinghe N, et al. Lens vault, thickness, and position in Chinese subjects with angle closure. *Ophthalmology.* 2011;118:474–479.
12. Nongpiur ME, Sakata LM, Friedman DS, et al. Novel association of smaller anterior chamber width with angle closure in Singaporeans. *Ophthalmology.* 2010;117:1967–1973.
13. Moghimi S, Vahedian Z, Zandvakil N, et al. Role of lens vault in subtypes of angle closure in Iranian subjects. *Eye.* 2014;28:337–343.
14. Guzman CP, Gong T, Nongpiur ME, et al. Anterior segment optical coherence tomography parameters in subtypes of primary angle closure. *Invest Ophthalmol Vis Sci.* 2013;54:5281–5286.
15. Nonaka A, Iwawaki T, Kikuchi M, Fujihara M, Nishida A, Kurimoto Y. Quantitative evaluation of iris convexity in primary angle closure. *Am J Ophthalmol.* 2007;143:695–697.
16. Sng CC, Allen JC, Nongpiur ME, et al. Associations of iris structural measurements in a Chinese population: the Singapore Chinese eye study. *Invest Ophthalmol Vis Sci.* 2013;54:2829–2835.
17. Foster PJ, Buhmann R, Quigley HA, Johnson GJ. The definition and classification of glaucoma in prevalence surveys. *Br J Ophthalmol.* 2002;86:238–242.
18. Moghimi S, Zandvakil N, Vahedian Z, et al. Acute angle closure: qualitative and quantitative evaluation of the anterior segment using anterior segment optical coherence tomography. *Clin Exp Ophthalmol.* 2014;42:615–622.
19. Méruła RV, Cronemberger S, Diniz Filho A, Calixto N. New comparative ultrasound biomicroscopic findings between fellow eyes of acute angle closure and glaucomatous eyes with narrow angle. *Arq Bras Oftalmol.* 2008;71:793–798.
20. Mimiwati Z, Fathilah J. Ocular biometry in the subtypes of primary angle closure glaucoma in University Malaya Medical Centre. *Med J Malaysia.* 2001;56:341–349.
21. Nongpiur ME, Gong T, Lee HK, et al. Subgrouping of primary angle-closure suspects based on anterior segment optical coherence tomography parameters. *Ophthalmology.* 2013;120:2525–2531.
22. Chylack LT, Wolfe JK, Singer DM, et al. The lens opacities classification system III. *Arch Ophthalmol.* 1993;111:831–836.
23. Casson RJ. Anterior chamber depth and primary angle-closure glaucoma: an evolutionary perspective. *Clin Exp Ophthalmol.* 2008;36:70–77.
24. Marchini G, Pagliaruso A, Toscano A, Tosi R, Brunelli C, Bonomi L. Ultrasound biomicroscopic and conventional ultrasonographic study of ocular dimensions in primary angle-closure glaucoma. *Ophthalmology.* 1998;105:2091–2098.
25. Bain W. The fellow eye in acute closed-angle glaucoma. *Br J Ophthalmol.* 1957;41:193–199.
26. Friedman DS, Chew P, Gazzard G, et al. Long-term outcomes in fellow eyes after acute primary angle closure in the contralateral eye. *Ophthalmology.* 2006;113:1087–1091.
27. Lowe RF. Acute angle-closure glaucoma: the second eye: an analysis of 200 cases. *Br J Ophthalmol.* 1962;46:641–650.
28. Mansouri M, Ramezani F, Moghimi S, et al. Anterior segment optical coherence tomography parameters in phacomorphic angle closure and mature cataracts: risk factors for phacomorphic angle closure. *Invest Ophthalmol Vis Sci.* 2014;55:7403–7409.
29. Sihota R, Dada T, Gupta R, Lakshminarayan P, Pandey RM. Ultrasound biomicroscopy in the subtypes of primary angle closure glaucoma. *J Glaucoma.* 2005;14:387–391.
30. Friedman DS, Gazzard G, Foster P, et al. Ultrasonographic biomicroscopy, Scheimpflug photography, and novel provocative tests in contralateral eyes of Chinese patients initially seen with acute angle closure. *Arch Ophthalmol.* 2003;121:633–642.
31. Lao YW, Hsieh JW, Hung PT. Ocular biometry in acute and chronic angle-closure glaucoma. *Ophthalmologica.* 2007;221:388–394.
32. Ang GS, Wells AP. Changes in Caucasian eyes after laser peripheral iridotomy: an anterior segment optical coherence tomography study. *Clin Exp Ophthalmol.* 2010;38:778–785.
33. He M, Friedman DS, Ge J, et al. Laser peripheral iridotomy in primary angle-closure suspects: biometric and gonioscopic outcomes: the Liwan Eye Study. *Ophthalmology.* 2007;114:494–500.
34. Kumar RS, Baskaran M, Chew PTK, et al. Prevalence of plateau iris in primary angle closure suspects: an ultrasound biomicroscopy study. *Ophthalmology.* 2008;115:430–434.
35. Yao B, Wu L, Zhang C, Wang X. Ultrasound biomicroscopic features associated with angle closure in fellow eyes of acute primary angle closure after laser iridotomy. *Ophthalmology.* 2009;116:444–448.